A Study on the High Resolution Infrared Spectra of an Asymmetric Top Molecule CF_2Cl_2

Hyun Chai Jung

Department of Chemistry, Kyung Hee University. Seoul 131-701. *Received March 21, 1988*

The high resolution IR spectra of freon-12(CF_2Cl_2) for the bands of 671cm^{-1}, 922cm^{-1}, 1102cm^{-1}, and 1160cm^{-1} were taken and the rotational vibrational analysis has been carried out. The band types of 671cm^{-1} and 1102cm^{-1} were confirmed to be A and those of 922cm^{-1} and 1160cm^{-1} were confirmed to be B. The theoretically synthesized spectra were matched with the experimentally obtained spectra to get some informations of the molecular rotational behavior as well as the overall band shape of the spectra.

Introduction

CF_2Cl_2 happens to belong to asymmetric top molecule, that causes the most researchers to have difficulties to handle the problems involved. So far only a few asymmetric top molecules were completely analyzed in band shape of infrared absorption spectra such as H_2O,[1] D_2O[2,3] and H_2S[4,5] etc. Band shape analysis of relatively large molecules such as CF_2Cl_2 was not attempted so often except by a few researchers such as Tompson and Temple,[6] Harold Jones,[14] and Gerhard Taubmann,[15] simply because so far the high resolution spectrophotometer was not good enough to resolve the individual rotational structure of the infrared absorption spectra of the freon R-12 molecules.

This work mainly concerned the theoretical band shape of the high resolution infrared absorption spectra of freon R-12 molecule. The molecular configuration of freon R-12 molecule has been taken from the Brockway's work.[7,8] The theoretical backgrounds have been adopted from the Allen and Cross' work.[9] Neglecting the centrifugal distortion and the coriolis effect, purely rigid rotor model was taken, so that the asymmetry parameter was taken fixed no matter how highly rotationally excited.

Our work is expected to be a basic work for the further research for the condensation and vaporization behavior through the high resolution infrared technique. Theoretically synthesized spectra were finally compared with the experimentally obtained spectra and discussed about the match. The B type band has shown multipeaked Q branches in this theoretically synthesized spectra instead of only two peaks, which were asserted by the previous workers[6] and the experimentally obtained spectra proved to be matched accordingly. The distinction between A and C type bands was clearly shown as a sharp and a broad Q branch respectively in this theoretically obtained spectra and yet the experimentally obtained spectra did not distinguish the differences.

In general the theoretical maneuvering to dig out the energy levels and intensities leads the author to understand the complex relationships between the asymmetry parameter and the spectral band shape and consequently being able to utilize the technique to any type or any size of the gas molecule for the investigation of either the molecular parameter and configuration or the band shape analysis.

Theory

In order to understand the high resolution vibration-rotation spectra of asymmetric top molecule (CF_2Cl_2), it is necessary to know the detail informations of the molecular vibrational and rotational energy levels.

Table 1. The Coefficients for the Matrix Elements of $E(K)$

representation	I^r	II^r	III^r
F	$1/2(K-1)$	0	$1/2(K+1)$
G	1	K	-1
H	$-1/2(K+1)$	1	$1/2(K-1)$
G-H	$-1/2(K-3)$	K	$-1/2(K+3)$
F+G-H	$K+1$	$K-1$	0
F+G+H	0	$K+1$	$K-1$

The asymmetric rotor,[10-12] $I_A \neq I_B \neq I_C$, is the most general case. The degree of asymmetry for an asymmetric top molecule is commonly measured by a dimensionless parameter K which is defined in terms of the rotational constants A,B, and C (in cm^{-1});

$$K=\frac{2B-A-C}{A-C} \qquad -1<K\leqq+1 \tag{1}$$

has the limiting values of -1 for a prolate symmetric top ($B = C$) and $+1$ for an oblate top ($A = B$) molecule. $K = 0$ corresponds to the most asymmetric case where $B = 1/2(A + C)$.

The energy level of an asymmetric top molecule can be written as;

$$E(A,\ B,\ C)=F(J,\tau)=\frac{A+C}{2}J(J+1)+\frac{A-C}{2}E_\tau(K)$$
$$\tau=1,2\cdots\cdots\cdots\cdots,2J+1 \tag{2}$$

$E(K)$ is essentially the energy of a molecule with inertial constants 1, K, and -1. As such, $E(K)$ can be calculated from the matrix elements of the Hamiltonian by making the appropriate substitutions. The matrix element of $E(K)$ may be written as;

$$(J,K,M|E(K)|J,K,M)=F[J(J+1)-K^2]+GK^2$$
$$=FJ(J+1)+(G-F)K^2 \tag{3}$$

$$(J,K,M|E(K)|J,K+2,M)=(J,K+2,M|H|J,K,M)$$
$$=H[f(J,K+1)]^{\frac{1}{2}} \tag{4}$$

Where the $f(J,K+1)$ are given by

$$f(J,n)=f(J,-n)=\frac{1}{4}[J(J+1)-n(n+1)]X$$
$$[J(J+1)-n(n-1)] \tag{5}$$

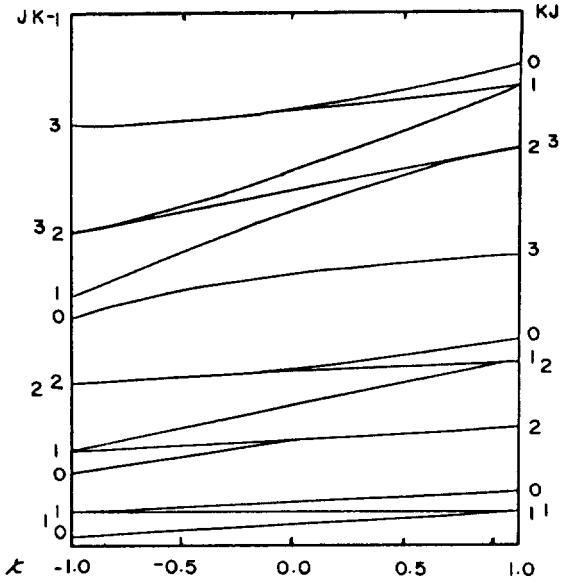

Figure 1. A plot of $E(K)$ versus K asymmetry parameter for low J's.

The expressions for F,G, and H in terms of K for the three right-handed representation are given in Table 1.

For an oblate spheroid, $I_A = I_B$, $A = B$, $K = 1$ and $Z = C$ (Type III), the energy matrix becomes diagonal; that is, $H = 0$. The matrix elements of $E(K)$ $E(1)$ becomes

$$\langle J, K, M | E(K) | J, K, M \rangle = J(J+1) - 2K_1^2 \tag{6}$$

Substitution of eq. (6) into eq. (2) yields eq. (9). For K in the neighborhood of +1, Type III representations are nearly diagonal, and hence the most conveniently used in determining the energy levels.

For the prolate limit $I_b = I_c$, $B = C$, $K = -1$, and $A = Z$ (Type I), the energy matrix is again diagonal, the elements being

$$\langle J, K, M | E(K) | J, K, M \rangle = -J(J+1) + 2K_{-1}^2, \tag{7}$$

giving eq. (8) when eq. (7) is substituted into eq. (2). Type 2, being nearly diagonal for K nearly -1, is the most convenient representation to use in this region of K.

Type 2 representations never become diagonal. Their main use is for maximum asymmetry $K = 0$. Here its main diagonal elements are all zero. The energy level diagram of $E(K)$ versus K asymmetry parameter is represented in Figure 1 for low J's.

The energy equations of the case one (prolate symmetric top) and case two (oblate symmetric top) can be written as;

$$\text{prolate top}: F(J, K) = CJ(J+1) + (A - C)K_{-1}^2, \tag{8}$$

$$\text{oblate top}: F(J, K) = AJ(J+1) + (C - A)K_1^2 \tag{9}$$

Where J,K are the quantum number, A,B and C are the rotational constants, K_{-1} and K_1 are the K quantum number.

The aymmetric top wave functions may be written as:

$$\psi_{JKM}^{(\theta,\phi,\chi)} = \theta_{JKM} e^{iK\chi} e^{iM\phi}$$

where $$\theta_{JKM}^{(\theta)} = N_{JKM} X^{\frac{1}{2}|K-M|} (1-X)^{\frac{1}{2}|K+M|} \sum_{\nu=0}^{n} a_\nu X^\nu \tag{10}$$

with

$$n = J - \frac{1}{2}|K+M| - \frac{1}{2}|K-M| \text{ and } X = \frac{1}{2}(1-\cos\theta)$$

Table 2. The Character table of V(x,y,z) group

	E	C_2^z	C_2^y	C_2^x
A	1	1	1	1
B_c	1	1	-1	-1
B_b	1	-1	1	-1
B_a	1	-1	-1	1

The ψ's of eq. (10) exists only for $J \geq K$, $J \geq M$. In the following, it is to be understood that the positive, numerical factor $N_{J,K,M}$ is such that $\psi_{J,K,M}$ is normalized, and the leading term of the Jacobi polynomial $\theta_{JKM}(\theta)$ has been taken as +1. In order always to have the correct phase, a suggestion originally made by Van Vleck[9] is followed by defining for $K = 0$

$$\phi_{J,K,M}^{\chi} = (-1)^{\beta} \psi_{J,K,M} \tag{11}$$

where $\beta = \frac{1}{2}|K+M| + \frac{1}{2}|K-M|$.

Furthermore, the function can be defined as;

$$S(J, K, M, \gamma) = 2^{-\frac{1}{2}}[\phi_{J,K,M}^{\chi} + (-1)^{\gamma}\phi_{J,-K,M}^{\chi}]$$
$$S(J, O, M, O) = \psi(J, O, M, O) \tag{12}$$

where may be even or odd, say 0 or 1, and for only even exists. If $K = 0$, there is one symmetric top wave function $\psi_{J,O,M}$ for each value of J,M. This belongs to the symmetric rotor species Σ_1, or Σ_2, depending on whether J is even or odd. If $K > 0$, species π, Δ, ect., there are two wave functions of equal energy for each J,M. These may most conveniently be taken either as $\psi_{J,K,M}$ and $\psi_{J,-K,M}$ of eq. (10) or as the two functions $S(J,K,M,\gamma)$ of eq. (12). Each asymmetric rotor wave function $A_{J,\tau,M}$ may be expressed as a linear combination of the symmetric rotor functions. These linear combinations assume the simplest form if we build them from the $S(J,K,M,\gamma)$'s. This is true because each $S(J,K,M,\gamma)$ satisfies the requirements for classification under a definite asymmetric rotor species which is not true for the (J,K,M)'s.

Under these conditions the wave function can be written as;

$$A(J, \tau, M) = \sum_{K\gamma} a_{K\gamma}^{JM} S(J, K, M, \gamma) \tag{13}$$

Since any $A(J,\tau,M)$ belongs to one of the four species of the V group, only $S(J,K,M,\gamma)$'s of that particular species have nonvanishing a's in eq.(13). In general, there will be several different $A(J,\tau,M)$ of the same species characterized by different sets of a's, hence the additional index τ. If two moments of inertia of an asymmetric rotor approach equality, and if the $S(J,K,M,\gamma)$'s of the nearest symmetric rotor case are used in eq.(13), then one $a_{K\gamma}^{JM}$ approaches unity and the others zero. Thus for every $A(J,K,M,\gamma)$ which it closely approximates. These new basis functions $S(J,K,M,\gamma)$ have been constructed relative to arbitrary axes x,y,z and not relative to the axes a,b,c of the molecule. They are therefore characterized by the representations A, B_a, B_b, B_c of the four group $V(x,y,z)$. The representations have been labeled to show directly the axis of rotation for which the character is +1. The character table of V group is given in Table 2.

The rotational-vibrational bands of an asymmetric rotor are even more complex than those of a symmetric rotor. The structure and analysis of asymmetrtic rotor bands is discussed in three type (A,B,C type). If the change in electric

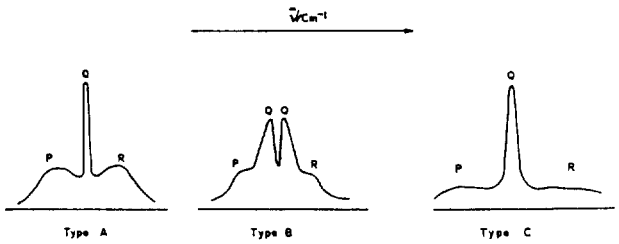

Figure 2. Typical band structures for asymmetric top molecule.

moment during a transition lies along the axis of least moment of inertia, the resulting band is called an A-type band. The selection rules for the strong transitions in an asymmetric rotor A-type band can be written as;

$$K_{-1}=0,\ \Delta J=\pm 1,\ \Delta K_{-1}=0,\ \Delta K_1=\pm 1$$
$$K_{-1}=0 \quad \Delta J=0,\pm 1 \quad \Delta K_{-1}=0 \quad \Delta K_1=\pm 1 \qquad (14)$$

These transitions would be expected to be strong because they are allowed in both symmetric rotor limits.

A C-type band results when the electric moment change during the vibrational transition is along the principal axis of largest moment of inertia. Such a change corresponds to a parallel band in the oblate symmetric limit and a perpendicular band in the prolate symmetric limit. Thus in a manner entirely analogous to that used for the A-type band, the following selection rules are represented for the strong transitions in the sub-bands of a C-type band;

$$\Delta J=\pm 1 \quad \Delta K_{-1}=\pm 1 \quad \Delta K_1=0 \quad K_1=0$$
$$\Delta J=0,\pm 1 \quad \Delta K_{-1}=\pm 1,\ \Delta K_1=0 \quad K_1=0 \qquad (15)$$

A B-type band arises when the change in electric moment during a vibration is along the principal axis of intermediate moment of inertia in both the prolate and the oblate symmetric limits the B-axis is perpendicular to the top axis; thus in both the symmetric rotor limits a B-type band corresponds to a perpendicular band. The selection rules for the strong transitions of a B-type band can be represented from those in the two symmetric limits.

$$\Delta J=0,\pm 1 \quad \Delta K_{-1}=\pm 1 \quad \Delta K_1=\pm 1 \qquad (16)$$

In general, the three type are represented as Figure 2

The theoretical high resolution vib-rotational spectra can be obtained by frequency calculation of the energy levels and their intensity calculations.

Experiments

Instrument. The instrument used for this work was Perkin Elmer Infrared Spectrophotometer E-14. The cell part of the instrument was deviced such that the freon R-12 can be injected into the cell through a pipe line from the freon R-12 gas bomb. Before the injection of the freon R-12 gas, the cell was evacuated by a vacuum pump (10^{-4} mmHg). The temperature of the gas in the cell was controlled by the thermostated heating or cooling water, which surrounded the cell.

The window material of the cell was KRS 5(Thallium bromide iodide), which well transmit the infrared spectral range from 400 cm^{-1} to 5000 cm^{-1}. The path length of the cell was 25 cm.

The spectral resolution was between 0.3 cm^{-1} and 0.5 cm^{-1} in the gas pressure range of 6 torr and 10 torr with slit width around 500μ.

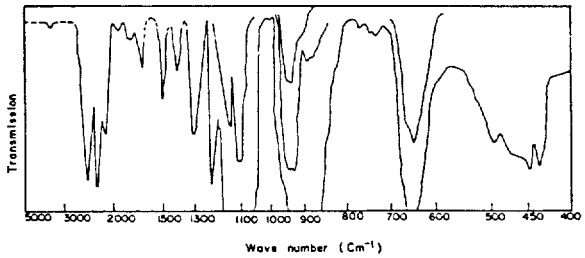

Figure 3. The IR-spectrum of CF_2Cl_2 from 400 Cm^{-1} to 5000 Cm^{-1}. (p = 10 Torr).

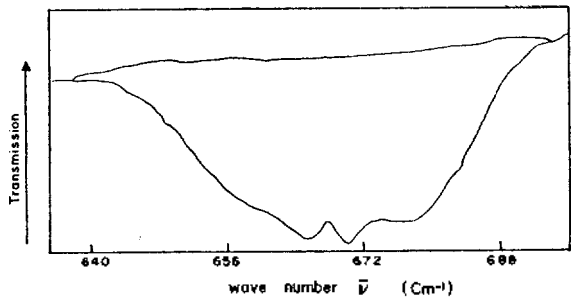

Figure 4a. The obtained IR-spectrum of CF_2Cl_2 at 671 Cm^{-1}. (p = 6 Torr).

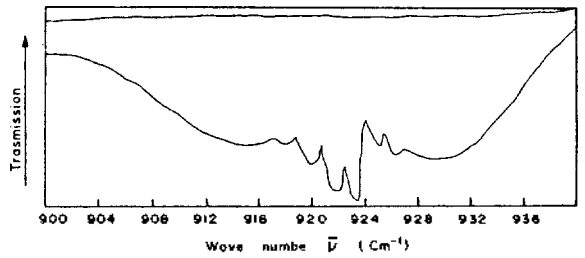

Figure 4b. The obtained IR-spectrum of CF_2Cl_2 at 922 Cm^{-1}. (p = 6 Torr).

Sample. The refrigerant freon R-12, specially purified by fractional distillation, was obtained from the Hoechst Company in Frankfurt, West Germany. The purity of the sample was 99.8%. The most likely impurities were stated to be $CClF_3$, $CFCl_3$ and $CHClF_2$, and the minimum amounts detectable by infrared analysis were 0.02, 0.01 and 0.05%, respectively.

The sample was redistilled twice in vacuum and finally distilled into the evacuated bomb, and then pumped into the cell, whose temperature was controlled by the thermostated heating or cooling water during the measurement, so that the inner pressure of the freon R-12 was maintained at the given value without much fluctuation.

Obtained Spectra. The infrared spectra of freon R-12 have been measured in the region 400 cm^{-1} to 5000 cm^{-1}. At room temperature, the sample was in the vapor state. The pressure of the vapor was that of the saturated vapor at room temperature (6 atm). The general spectra was appeared in the Figure 3.

The high resolution spectra of freon R-12 was measured at room temperature and between the 1 torr and 10 torr pressure. The spectral resolution was measured with the accuracy between 0.3 cm^{-1} and 0.5 cm^{-1}. The high resolution spectra of 671 cm^{-1}, 922 cm^{-1}, 1102 cm^{-1}, 1160 cm^{-1} were appeared in the Figure 4a, Figure 4b, Figure 4c and Figure 4d.

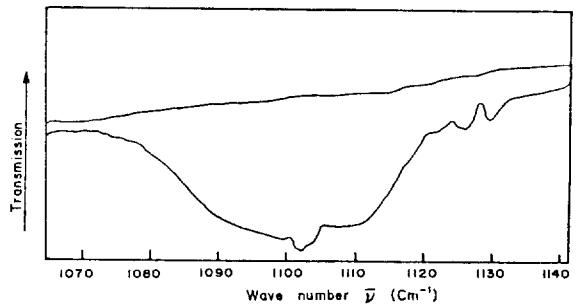

Figure 4c. The obtained IR-spectrum of CF_2Cl_2 at 1102 Cm^{-1}. (p = 6 Torr).

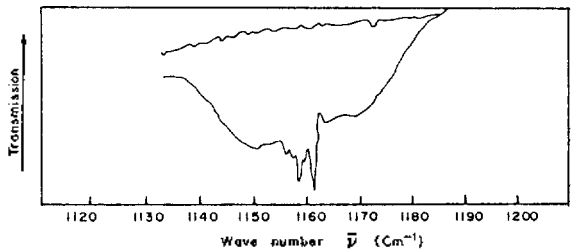

Figure 4d. The obtained IR-spectrum of CF_2Cl_2 at 1160 Cm^{-1}. (p = 6 Torr).

Table 3. The Observed Vibrational Frequences in the Gaseous State

Previous Raman data (cm^{-1})	Present Infrared data (cm^{-1})	Interpretation
261.5	–	fundamental
322	–	fundamental
433	–	fundamental
457.5	–	fundamental
667.2	671(strong)	fundamental
877	882(strong)	fundamental
923	922(very strong)	fundamental
1098	1102(strong)	fundamental
1167	1160(strong)	fundamental

Discussion

Analytical Results. The Raman spectrum of freon R-12 was measured by Claassen.[13] The infrared spectrum is shown in Figure 3 and Figure 4. The important positions of the bands are given in Table 3.

The freon R-12 (CF_2Cl_2) falls into the symmetry point group C_{2v}. The nine fundamental modes of C_{2v} are appeared in the Figure 5 and form four groups, indicated in Table 4.

Comparison of theoretical and experimental spectra. The theoretically calculated spectra through the computer programming (Appendix) are given in Figure 6a, Figure 6b and Figure 6c. The *A*,*B* and *C* types are shown self-evidently distinguishable one another in the Figures. The characteristic of the A-type represent the rather broad *P* and *R* branch with the very sharp central *Q* branch. The characteristic of the C-type is similar to the A-type, but a little bit broader *Q* shape than A-type.

Thomson and Temple[6] once discussed the band shapes. Their conclusions with the Badger, Zurmwalt and R.S. Rasmussen's computations suggested that the B-type bands will have four sub-maxima with central spacing about 5 cm^{-1} and outer spacing about 13 cm^{-1} and the A-type and C-type bands will each have three sub-maxima with outer spacings of about 15 cm^{-1} and 20 cm^{-1}.

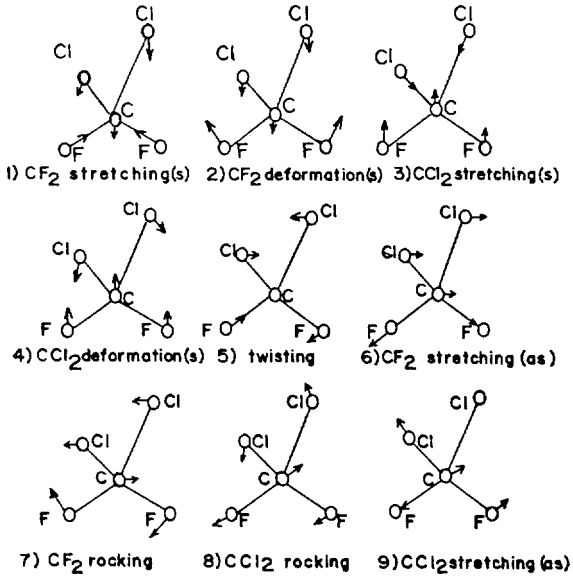

Figure 5. The nine fundamental vibrations of CF_2Cl_2.

Table 4. The Nine Fundamental Modes of CF_2Cl_2

Symmetry w.r.t. Class	C_2	σ_x	σ_y	Infra-red	No. of modes	Nature of Vibration
A_1	s	s	s	Mz	4	Symm. CCl_2 stretching Symm. CF_2 stretching Symm. CCl_2 deformation Symm. CF_2 deformation
A_2	s	as	as	ia	1	Twisting
B_1	as	as	s	Mx	2	Antisymm. CCl_2 stretching rocking
B_2	as	s	as	My	2	Antisymm CF_2 stretching rocking

Our calculated spectra show some more detailed structure of each type which Thomson and Temple had described. For the B-type, the central two peaks by the Thomson and Temple must belong to *Q* branches, which might resolve further such that multi peaks might appear as shown in our obtained spectra 922 cm^{-1} and 1160 cm^{-1}. The *Q* branch for A-type and C-type can be distinguished by their band with, i.e., our computed analysis indicate that the C-type *Q* branch must be much broader than A-type *Q* branch. Unfortunately our obtained spectra was not clearly showing this differences, but if we were able to get a better high resolution spectra, *A* and C-type *Q* branches could be distinguished by relative band width.

The experimentally obtained spectra are in the Figure 4a, Figure 4b, Figure 4c and Figure 4d. The 671 cm^{-1} and 1102 cm^{-1} bands which were shown in Figure 4a and Figure 4c are more or less like A-type or C-type. The 92 cm^{-1} and 1160 cm^{-1} bands which were shown in Figure 4b and Figure 4a are B-type.

With close examination of the obtained spectra compared

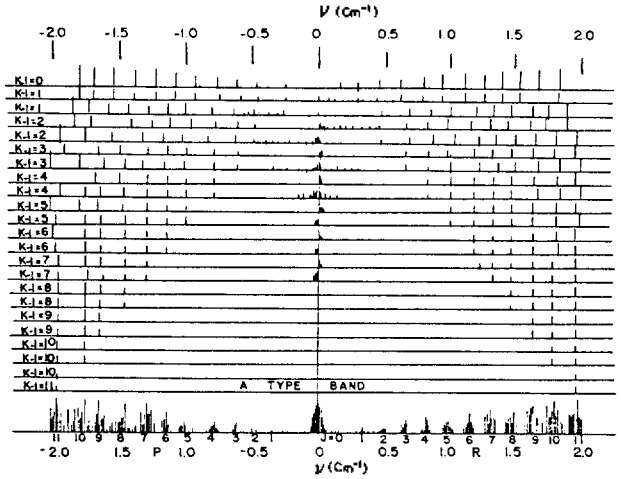

Figure 6a. The A-type band of the theoretically calculated spectra for CF_2Cl_2.

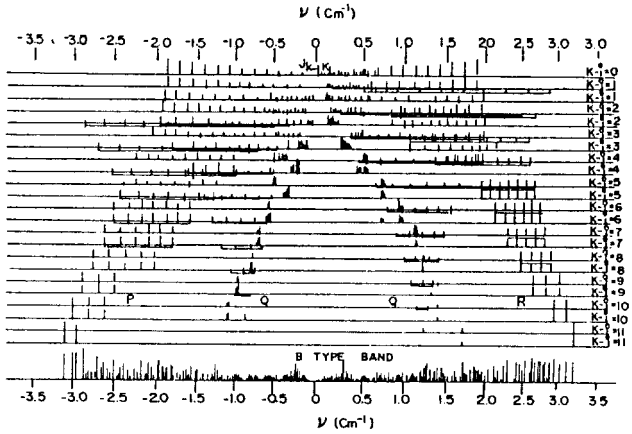

Figure 6b. The B-type band of theoretically calculated spectra for CF_2Cl_2.

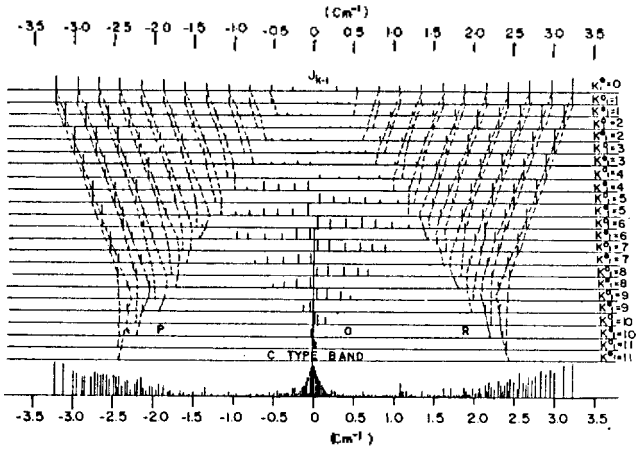

Figure 6c. The C-type band of theoretically calculated spectra for CF_2Cl_2.

with the theoretically calculated ones, we concluded that the 671 cm^{-1} and 1102 cm^{-1} bands were A-type or C-type, and the 992 cm^{-1} and 1160 cm^{-1} bands were B-type.

Conclusion

The resolution of the instrument was between 0.3 cm^{-1}, and 0.5 cm^{-1}, which was not good enough to resolve the detail rotational levels so that the each single rotational lines were not able to be identified with proper quantum number.

The light source was not strong enough so that the absorption spectrum was not resolved clearly at the lower pressure of the sample. Even for the *P* and *R* branches, particulstly *Q* branch, there was no way to be resolved for the identification with the proper quantum number.

The spectral shape was rather sensitive to the pressure. In order to resolve the single rotational lines, the lower pressure of the sample and the stronger light source were recommended.

Even with the above difficulties, the authors attempt to distinguish the band type was rather successful. Especially, the four bands were identified such that the 671 cm^{-1}, 1102 cm^{-1} were A-type or C-type and the 922 cm^{-1}, 1160 cm^{-1} were B-type, which were previously somewhat target of argument among the previous workers on the freon R-12 problems.

The process of theoretical computation leads to see the insight of the molecular rotational behavior and distinct way to predict the spectra. But because of the poor experimental apparatus, the desirable accuracy was unfortunately missed. Even though, the brief idea of getting the information of the molecular rotational behavior was understood.

The band shape analysis was worthwhile to recognize the overall shape of the spectra through the comparison of the theoretically calculated spectra with the experimentally obtained spectra. Each quantum number identification was not easy but can be estimated on the not resolved experimental spectra by careful examination. These tedious processes may lead to understand the pressure broadening of the line shape. The author hopes that the pressure effect on the rotational suructure of the spectra may give a chance to investigate the Joule-Thomson effect in the molecular dimension. The pressurizing and expansion behavior of the freon R-12 molecule can be studied more intensively through the spectroscopic data processing. This work has been pursued to help understand the basic knowledge for the pressure effect on the molecular rotation. Further detailed work of the pressure effect on the molecular rotation will be a subject of further work.

Acknowledgement. The auther expresses thanks to the Korean Government, Ministry of Education, that financially supported the work.

References

1. H. H. Nielsen, *Physical Review*, **59**, 565 (1941).
2. G. W. King, *J. Chem. Physic*, **15**, 85 (1947).
3. P. A. Giguere, *J. Chem. Physic*, **19**, 1086 (1951).
4. H. C. Allen and P. C. Cross, *J. Chem. Physic*, **18**, 691 (1950).
5. R. M. Hainer and G. W. King, *J. Chem. Physic*, **15**, 89 (1947).
6. H. W. Thompson and R. B. Temple, *J. Am. Chem. Soc.*, **70**, 1422 (1948).
7. L. O. Brockway, *J. Am. Chem. Soc.*, **58**, 185 (1936).
8. L. O. Brockway, *J. Am. Chem. Soc.*, **58**, 747 (1936).
9. H. C. Allen and P. C. Cross, Molecular Vib-Rotors; The Theory and interpretation of high resolution infrared spectra, New York: John Wiley and Sons, 1936.

10. G. W. King, R. M. Hainer and P. C. Cross, *J. Chem. Physic*, **11**, 27 (1943).
11. P. C. Cross, R. M. Hainer and G. W. King, *J. Chem. Physic*, **12**, 210 (1944).
12. R. S. Mulliken, *J. Chem. Physic*, **59**, 873 (1941).
13. H. H. Claassen, *J. Chem. Physic*, **22**, 50 (1954).
14. J. Harold and M.-C. Mireile, *J. Mol. Spec.*, **91**, 87 (1982).
15. T. Gerhard and J. Harold, *J. Mol. Spec.* **117**, 283 (1986).

Magnetic and Electrical Properties of High-Tc Superconductor $YBa_2Cu_3O_{6.87}$

Don Kim, Chang Kwon Kang, Keu Hong Kim*, and Jae Shi Choi

Department of Chemistry, Yonsei University, Seoul 120-749. *Received March 28, 1988*

The structural, electrical and magnetic properties were investigated for the high-T_c superconductor $YBa_2Cu_3O_{7-x}$ where x was 0.13. The results of temperature dependence of the resistivity and the magnetization in $YBa_2Cu_3O_{6.87}$ whose structure and phase are confirmed by analysis of X-ray powder diffraction pattern have been reported. A very sharp superconductivity transition appears at 92K in the specimen whose chemical composition is determined from redox titration, strongly suggesting that this specimen consists of a single-phase superconductor. From the results of X-ray diffraction analysis, magnetization curves, levitation and resistance measurements, it is suggested that the observed superconductivity is bulk property in nature and that the $YBa_2Cu_3O_{6.87}$ phase is responsible for the superconductivity of the present reproducible specimen.

Introduction

Extensive studies have been made to clarify the nature of the high-T_c superconductivity, since Bednorz and Muller[1] reported possible high-T_c superconductivity in the Ba-La-Cu-O system. At ambient pressure a stable superconducting transition temperature between 77 and 93 K has been observed in Y-Ba-Cu-O systems[2,3]. Even for the Y-Ba-Cu-O system of the same composition, the magnetic and electrical properties vary depending on the method of specimen preparation. A mixing process of starting materials, sintering temperature and time, and cooling rate are expected to be important for obtaining homogeneous high-T_c superconductors. Although the diamagnetism due to the superconductivity has been reported by Wu *et al.*[2], the magnetic susceptibility has reached only about 25% of the complete Meissner effect. In the temperature dependence of the magnetic susceptibility, a great variety of specimen characteristics has been observed and reported around 90 K, depending on the sintering condition and starting composition[2,4]. From the resistivity and magnetic susceptibility data, it is suggested that the multi-phase in Y-Ba-Cu-O system exists even in the case that sharp superconducting transition is observed in resistance at around 90 K. Since the magnetic susceptibility is essential for the superconductivity and is sensitive to the multiphase, the magnetization curve in the low and the high fields is useful and important not only in the new scientific information concerning the high-T_c superconducting mechanism but also in the field of industrial applications. However, the full value of diamagnetic susceptibility expected from the Meissner effect was not observed, since impurity phases may exist in high-T_c superconductor. In the very recent experimental results, surprising results are in the high-T_c magnetic superconducting oxides[5,6]. Although the rare-earth ions are magnetic, rare-earth ions-Ba-Cu-O systems are still comparable in T_c with that of Y-Ba-Cu-O systems. The present work aims at synthesizing the reproducible high-T_c superconductor, refining its crystal phase, and determining the magnetic and electrical properties. In continuous work we will try to synthesize a new high-T_c superconductor which shows dry-ice transition temperature.

Experimental

Sample preparation and analysis. $YBa_2Cu_3O_{6.87}$ was prepared by an ordinary powder metallurgy technique. Starting powder materials of Y_2O_3(99.99%, Aldrich Co.), $BaCO_3$ (99.999%, Aldrich Co.) and CuO(99.999%, Aldrich Co.) were ball-mill-mixed and calcined at 880 °C for 10 hours in air. The well mixed powder was pressed into a pellet by 49 MPa and the pellet was sintered at 920 °C for 17 hours in air and then annealed at 700 °C for 12 hours. After annealing, specimen was furnace-cooled to room temperature in air at a cooling rate of 50 °C/hr. X-ray spectra obtained by a diffractometer (Philips, PW 1710, CuK_α) identified the specimen as an essential simple phase of the layered perovskite structure. The high-T_c superconducting phase of present compound as an orthorhombic and oxygen-defect perovskite was found to be chemical composition $YBa_2Cu_3O_{6.87}$ from redox titration[7].

Magnetization and resistance measurements. A powder specimen was used for magnetization measurement. Magnetizations were measured by using a vibrating sample magnetometer (EG & G Princeton Applied Research Co., Model 135) in the fields up to 5 KG at 79 K. A specimen of about 1.3 mm × 5 mm × 12 mm in size was cut from the pellet and was used for resistance measurements. For the resistance measurements, a standard four-probe AC and DC methods were employed and a silver paste(Dupont Co. 4929) was used as contact material. Platinum wires were used as electrical leads and were attached to the sample with conducting silver paste. The current density used for the measurement of electrical resistance was between 1 mA/cm^2 and 10 mA/cm^2, and resolution of the voltage measurement was 1×10^{-8}V. The resistance and transition temperature were